*JOURNAL OF GEOPHYSICAL RESEARCH - BIOGEOSCIENCES*

Supporting Information for

# Trees talk tremor – Wood anatomy and $\delta^{13}C$ content reveal contrasting tree-growth responses to earthquakes

Christian H. Mohr[1], Michael Manga[2], Gerhard Helle[3], Ingo Heinrich[3], Laura Giese[4], Oliver Korup[1]

[1]Institute of Environmental Sciences and Geography, University of Potsdam, Germany

[2]Department of Earth and Planetary Science, University of California, 307 McCone Hall, Berkeley, CA 94720, USA

[3]GFZ German Research Centre for Geosciences, Telegrafenberg, 14473 Potsdam, Germany

[4]German Federal Institute of Hydrology (BfG), 56002 Koblenz, Germany

## Contents of this file

Text S1 to S2
Figures S1 to S11
Tables S1 to S7

## Additional Supporting Information (Files uploaded separately)

| Name | Tree ID | Growing Season | Parameter |
|---|---|---|---|
| NacPi6_2007_iso | NacPi6 | 2006-2007 | $\delta^{13}C_{OM}$ |
| NacPi6_2008_iso | NacPi6 | 2007-2008 | $\delta^{13}C_{OM}$ |
| NacPi6_2009_iso | NacPi6 | 2008-2009 | $\delta^{13}C_{OM}$ |
| NacPi6_2010_iso | NacPi6 | 2009-2010 | $\delta^{13}C_{OM}$ |
| NacPi6_2011_iso | NacPi6 | 2010-2011 | $\delta^{13}C_{OM}$ |
| NacPi6_2012_iso | NacPi6 | 2011-2012 | $\delta^{13}C_{OM}$ |

| | | | |
|---|---|---|---|
| NacPi7_2008_iso | NacPi7 | 2007-2008 | $\delta^{13}C_{OM}$ |
| NacPi7_2009_iso | NacPi7 | 2008-2009 | $\delta^{13}C_{OM}$ |
| NacPi7_2010_iso | NacPi7 | 2009-2010 | $\delta^{13}C_{OM}$ |
| NacPi7_2011_iso | NacPi7 | 2010-2011 | $\delta^{13}C_{OM}$ |
| NacPi7_2012_iso | NacPi7 | 2011-2012 | $\delta^{13}C_{OM}$ |
| NacPi11_2008_iso | NacPi11 | 2007-2008 | $\delta^{13}C_{OM}$ |
| NacPi11_2009_iso | NacPi11 | 2008-2009 | $\delta^{13}C_{OM}$ |
| NacPi11_2010_iso | NacPi11 | 2009-2010 | $\delta^{13}C_{OM}$ |
| NacPi11_2011_iso | NacPi11 | 2010-2011 | $\delta^{13}C_{OM}$ |
| NacPi11_2012_iso | NacPi11 | 2011-2012 | $\delta^{13}C_{OM}$ |
| NacPi11_2013_iso | NacPi11 | 2012-2013 | $\delta^{13}C_{OM}$ |
| NacPi20_2007_iso | NacPi20 | 2006-2007 | $\delta^{13}C_{OM}$ |
| NacPi20_2008_iso | NacPi20 | 2007-2008 | $\delta^{13}C_{OM}$ |
| NacPi20_2009_iso | NacPi20 | 2008-2009 | $\delta^{13}C_{OM}$ |
| NacPi20_2010_iso | NacPi20 | 2009-2010 | $\delta^{13}C_{OM}$ |
| NacPi20_2011_iso | NacPi20 | 2010-2011 | $\delta^{13}C_{OM}$ |
| NacPi20_2012_iso | NacPi20 | 2011-2012 | $\delta^{13}C_{OM}$ |
| NacPi25_2010_iso | NacPi25 | 2009-2010 | $\delta^{13}C_{OM}$ |
| NacPi25_2011_iso | NacPi25 | 2010-2011 | $\delta^{13}C_{OM}$ |
| NacPi25_2012_iso | NacPi25 | 2011-2012 | $\delta^{13}C_{OM}$ |
| NacPi25_2013_iso | NacPi25 | 2012-2013 | $\delta^{13}C_{OM}$ |
| NacPi30_2008_iso | NacPi30 | 2007-2008 | $\delta^{13}C_{OM}$ |
| NacPi30_2009_iso | NacPi30 | 2008-2009 | $\delta^{13}C_{OM}$ |
| NacPi30_2010_iso | NacPi30 | 2009-2010 | $\delta^{13}C_{OM}$ |
| NacPi30_2011_iso | NacPi30 | 2010-2011 | $\delta^{13}C_{OM}$ |
| NacPi30_2012_iso | NacPi30 | 2011-2012 | $\delta^{13}C_{OM}$ |
| NacPi30_2013_iso | NacPi30 | 2012-2013 | $\delta^{13}C_{OM}$ |
| d13C_NacPi_annual | NacPi6, NacPi7, NacPi11, NacPi20, NacPi25, NacPi30 | 1987/88-2012/2013 | $\delta^{13}C_{OM}$ |
| nacpi6c_2008 | NacPi6 | 2007-2008 | Lumen area |
| nacpi6c_2009 | NacPi6 | 2008-2009 | Lumen area |
| nacpi6c_2010 | NacPi6 | 2009-2010 | Lumen area |
| nacpi6c_2011 | NacPi6 | 2010-2011 | Lumen area |

| | | | |
|---|---|---|---|
| nacpi6c_2012 | NacPi6 | 2011-2012 | Lumen area |
| nacpi6c_2013 | NacPi6 | 2012-2013 | Lumen area |
| nacpi7c_2008 | NacPi7 | 2007-2008 | Lumen area |
| nacpi7c_2009 | NacPi7 | 2008-2009 | Lumen area |
| nacpi7c_2010 | NacPi7 | 2009-2010 | Lumen area |
| nacpi7c_2011 | NacPi7 | 2010-2011 | Lumen area |
| nacpi7c_2012 | NacPi7 | 2011-2012 | Lumen area |
| nacpi7c_2013 | NacPi7 | 2012-2013 | Lumen area |
| nacpi11c_2008 | NacPi11 | 2007-2008 | Lumen area |
| nacpi11c_2009 | NacPi11 | 2008-2009 | Lumen area |
| nacpi11c_2010 | NacPi11 | 2009-2010 | Lumen area |
| nacpi11c_2011 | NacPi11 | 2010-2011 | Lumen area |
| nacpi11c_2012 | NacPi11 | 2011-2012 | Lumen area |
| nacpi11c_2013 | NacPi11 | 2012-2013 | Lumen area |
| nacpi20c_2008 | NacPi20 | 2007-2008 | Lumen area |
| nacpi20c_2009 | NacPi20 | 2008-2009 | Lumen area |
| nacpi20c_2010 | NacPi20 | 2009-2010 | Lumen area |
| nacpi20c_2011 | NacPi20 | 2010-2011 | Lumen area |
| nacpi20c_2012 | NacPi20 | 2011-2012 | Lumen area |

| | | | |
|---|---|---|---|
| nacpi20c_2013 | NacPi20 | 2012-2013 | Lumen area |
| nacpi25c_2007 | NacPi25 | 2006-2007 | Lumen area |
| nacpi25c_2008 | NacPi25 | 2007-2008 | Lumen area |
| nacpi25c_2009 | NacPi25 | 2008-2009 | Lumen area |
| nacpi25c_2010 | NacPi25 | 2009-2010 | Lumen area |
| nacpi25c_2011 | NacPi25 | 2010-2011 | Lumen area |
| nacpi25c_2012 | NacPi25 | 2011-2012 | Lumen area |
| nacpi25c_2013 | NacPi25 | 2012-2013 | Lumen area |
| nacpi30c_2008 | NacPi30 | 2007-2008 | Lumen area |
| nacpi30c_2009 | NacPi30 | 2008-2009 | Lumen area |
| nacpi30c_2010 | NacPi30 | 2009-2010 | Lumen area |
| nacpi30c_2011 | NacPi30 | 2010-2011 | Lumen area |
| nacpi30c_2012 | NacPi30 | 2011-2012 | Lumen area |
| nacpi30c_2013 | NacPi30 | 2012-2013 | Lumen area |

**DATA.** The filename is composed of the name given in the table and the ending".txt". Upper case is used for the $\boldsymbol{\delta^{13}C_{OM}}$ data (grey), while lower case is used for wood anatomic data. We are going to upload the data to a public repository, pending the final decision on this manuscript.

## Introduction

Our supporting material comprises a two text sections explaining in more detail the calculation of the topographical indices we considered (S1), and presenting an overview of our $\delta^{13}C_{OM}$ sample preparation in the lab. We provide additional figures showing intra-annual time series of wood anatomy (Figures S1.3-1.6) and $\delta^{13}C_{OM}$ (Figure S1.9). Further we provide a figure of residual lumen area signals the period for period 2008-2013 (Figure S1.1), the concentration of atmospheric $CO_2$ measured which the detrended

atmospheric $CO_2$ and modeled cellular $CO_2$ concentration build on (Figure S1.2). One additional figure depicts the modeled growing rates of *Pinus radiata* (Figure S.1.7), another one illustrates the inter-annual $\delta^{13}C_{OM}$ cellulose measurements of the cored trees (Figure S.1.8). Figure S1.10 provides an additional figure of the Southern Oscillation Index (SOI) and the cross-correlation with model residuals, while Figure S1.11 presents cumulative density functions of model residuals to allow for better context (also see Table S8 for values). The supporting information also comprises a table (Table S1) with field measurements of DBH and tree height growth from Nacimiento *Pinus radiata* plantation forests (data provided by Mininco), a table providing information on tree-specific numbers of $\delta^{13}C_{OM}$ samples. Table S3 provides model performance and relative variable importance of our Boosted Regression Tree approach. Table S4 and S5 present additional meteorological data and potential incoming solar radiation, respectively. Lastly, Tables S6 and S7 provide an overview of tree- and growing-season-specific wood anatomic proxies, and annually resolved $\delta^{13}C_{OM}$ values.
We also upload our intra-annually resolved $\delta^{13}C_{OM}$ and lumen area data to a public repository, pending the final decision on this manuscript.

**Text S1. Topographic variables**

We quantified topographic variables that explicitly account for subsurface hydrology: (1) topographic wetness index (TWI), (2) aspect, (3) distance from closest stream, (4) relative hillslope height, and (5) topographic position index (TPI). To this end we first resampled a 1-m airborne LiDAR DEM to 5-m horizontal resolution to reduce extreme values of the TWI and TPI estimates [*Jucker et al.*, 2018]. We averaged all site variables within a radius of 10 m around each tree to include the area of influence for root water uptake. Given an average tree crown diameter of <10 m [*Huber et al.*, 2010], this buffer value is motivated by observations that relate horizontal root spread and tree crown diameter [*Smith*, 1964]. Relative hillslope height refers to how near a sampled tree is to either valley bottom (0) or the ridge line (1) [*Conrad et al.*, 2015]. The TWI describes the tendency to accumulate subsurface water, though neglecting soil properties and capillarity effects [*Boehner et al.*, 2002; *Boehner and Selige*, 2006]:

$$\mathrm{TWI} = \ln\left(\frac{a}{\tan\beta}\right) \quad (1)$$

where $a$ is upslope accumulated area and $\beta$ is local slope *[Beven and Kirkby*, 1979]. The TPI measures relative topographic position as the difference between the elevation at a central point $Z_0$ and the mean elevation $\bar{Z}$ in a given neighborhood defined by a radius (R):

$$\mathrm{TPI} = Z_0 - \bar{Z} = Z_0 - \frac{1}{n_R}\sum_{i \in R} Z_i \quad (2)$$

where $Z_i$ is the elevation of the DEM grid and $n$ is the total number of surrounding pixels (n = 20) [Wilson and Gallant, 2000].

**Text S2. $\delta^{13}C_{OM}$ sample preparation**

We manually separated tree rings using a scalpel under a microscope. We extracted wood α-cellulose to avoid isotope variations caused by varying contents of other structural and non-structural wood fractions. We used sodium hydroxide, sodium chlorite and acetic acid to remove the extractives [*Loader et al.*, 1997] according to standard methodologies [*Schollaen et al.*, 2015; *Wieloch et al.*, 2011]. Then, we homogenized α-cellulose with an ultrasonic device and freeze-dried according to Schollaen et al. [2017], before we packed between 180 and 220 µg of cellulose into tin capsules.

First, cross-sections from the wood cores were cut with a core microtome. Second, the cross-sections (approx. 500 µm thick) were fixed in special metal frame slides and mounted on the object holder of the microdissection microscope. We used 40-80 µg of independent standards: Fluka-cellulose (100-150 µg), graphite V USGS24 and IAEA CH-7.

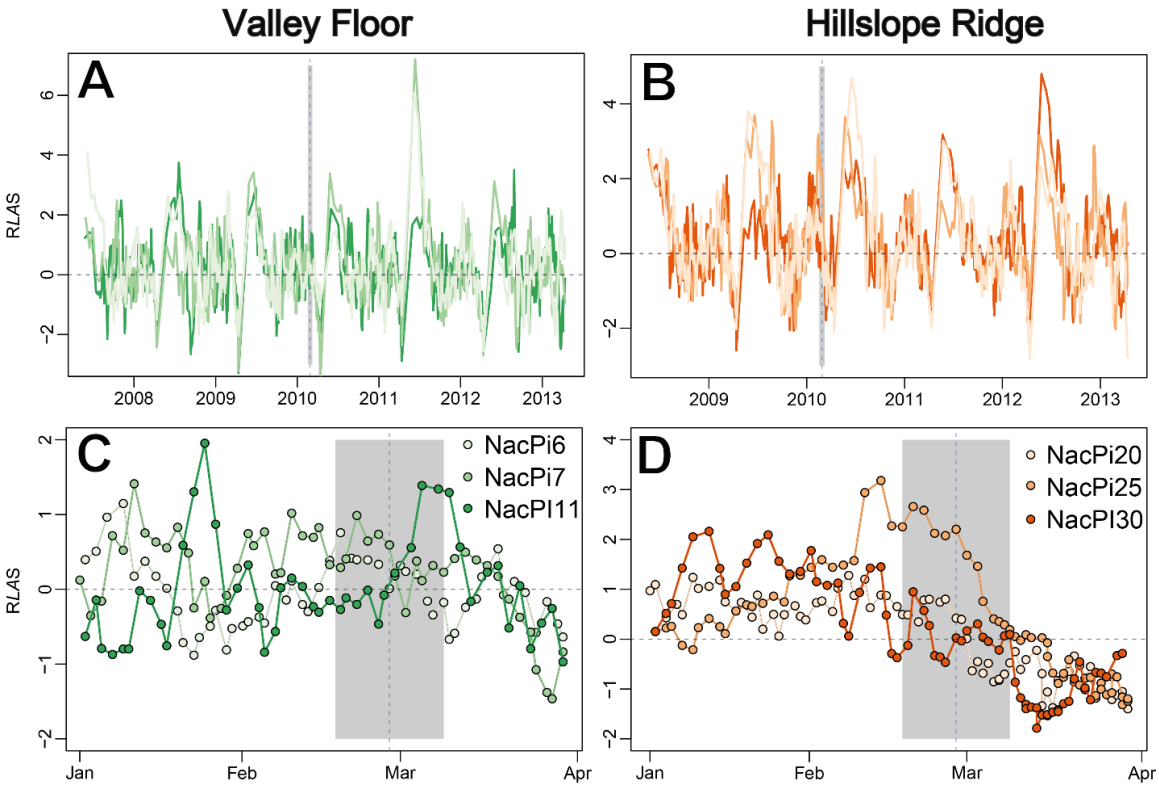


**Supplementary Figure 1.** Standardized *RLAS*, i.e. residual lumen area signals, for the period 2008-2013 (**a, b**) and January to April 2010 (**c, d**). Residuals refer to sinusoidal models fitted to each tree per each growing season (Figure 6 **c, d**). Green and red colors indicate single trees on the valley floor (A, B) and the ridge, respectively. Mean lumen area per tree was calculated over all eight tracheid paths. The grey bars and dashed lines show the time of the earthquake and a time window of ±10 days, respectively.

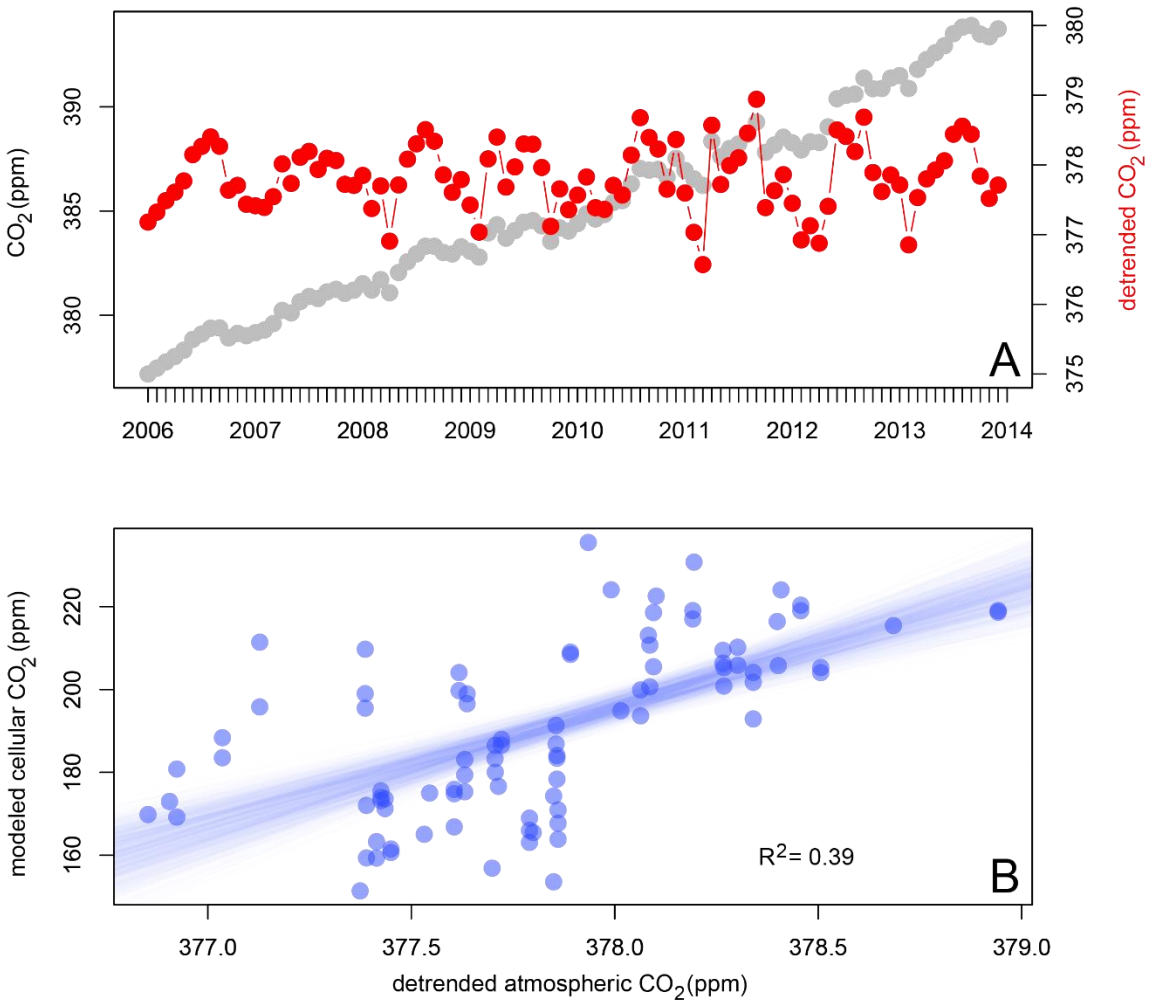


**Supplementary Figure 2.** A: Concentration of atmospheric $CO_2$ (grey dots) at Baring Head, New Zealand [*Keeling et al.*, 2001]. The red dots show detrended $CO_2$ concentration. B: Blue dots are measured detrended atmospheric $CO_2$ and modeled cellular $CO_2$ concentration for sample NacPi6 in 2008, 2009, 2011, and 2012. The light blue lines are $n$ = 10,000 bootstrapped median regression models with goodness of model fit given by $R^2$.

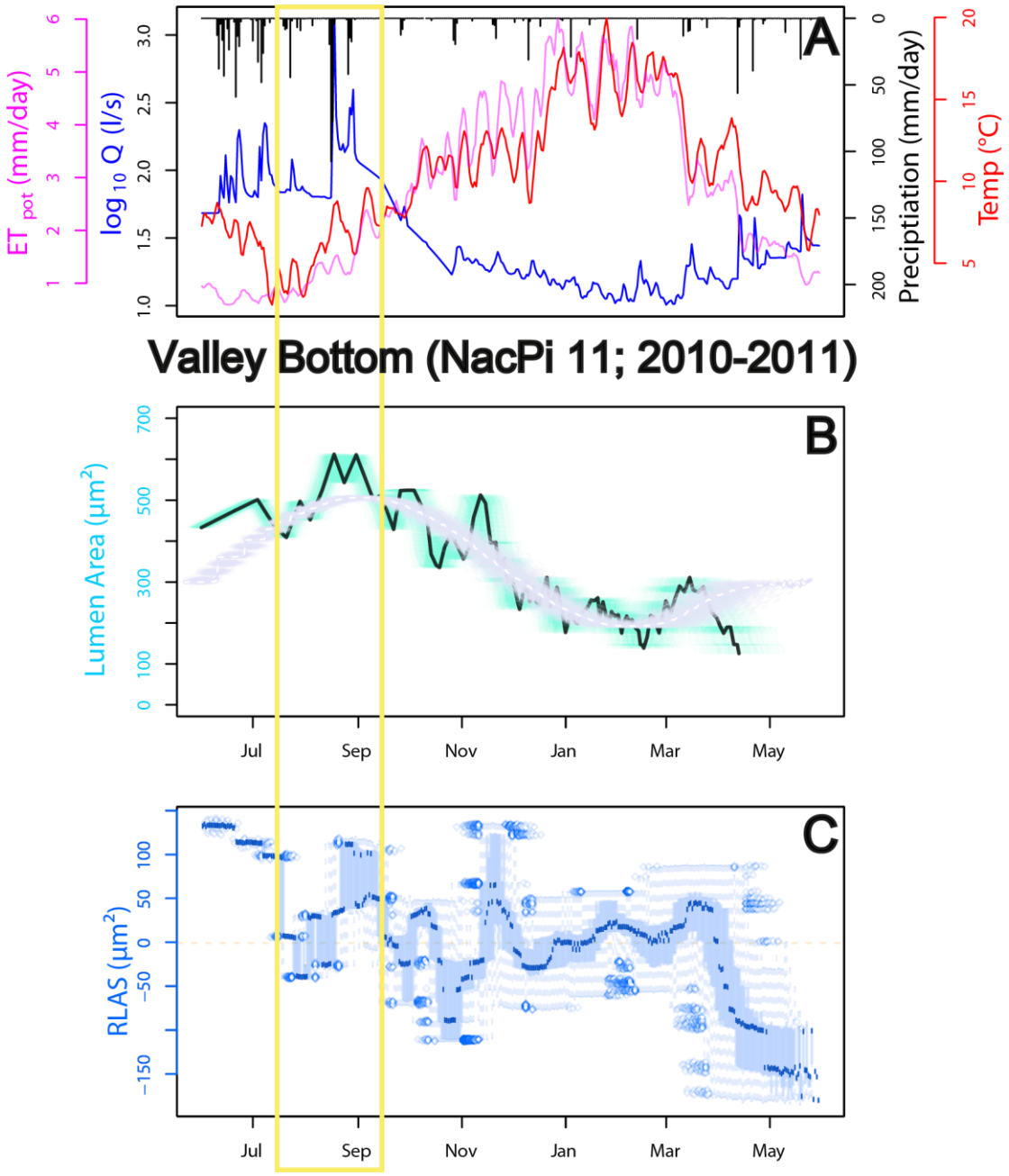


**Supplementary Figure 3. a)** Wood anatomy of NacPi11 for the 2010-11 growing season; streamflow discharge (in logarithmic scale) in blue, rainfall (black), and air temperature (red) for 06/2010-06/2011 measured in Pichún; Potential evapotranspiration (red lines) in Nicodahue catchment (#8362001) from the CAMEL-CL dataset [*Alvarez-Garreton et al.*, 2018]. **b)** The thick black curves are the medians of n = 10,000 MC-modeled time series of lumen area (green array of curves) and the white dashed lines are the medians of *n*=10,000 MC sine models from 06/2010 to 05/2011. **c)** The light blue boxplots are the *RLAS* binned to daily values, with the medians in dark blue. The orange bars and dashed lines mark the earthquake date ±10 days. The yellow box highlights a period where lumen area follows the rainfall and streamflow discharge patterns relatively closely (But see also Fig. S12).

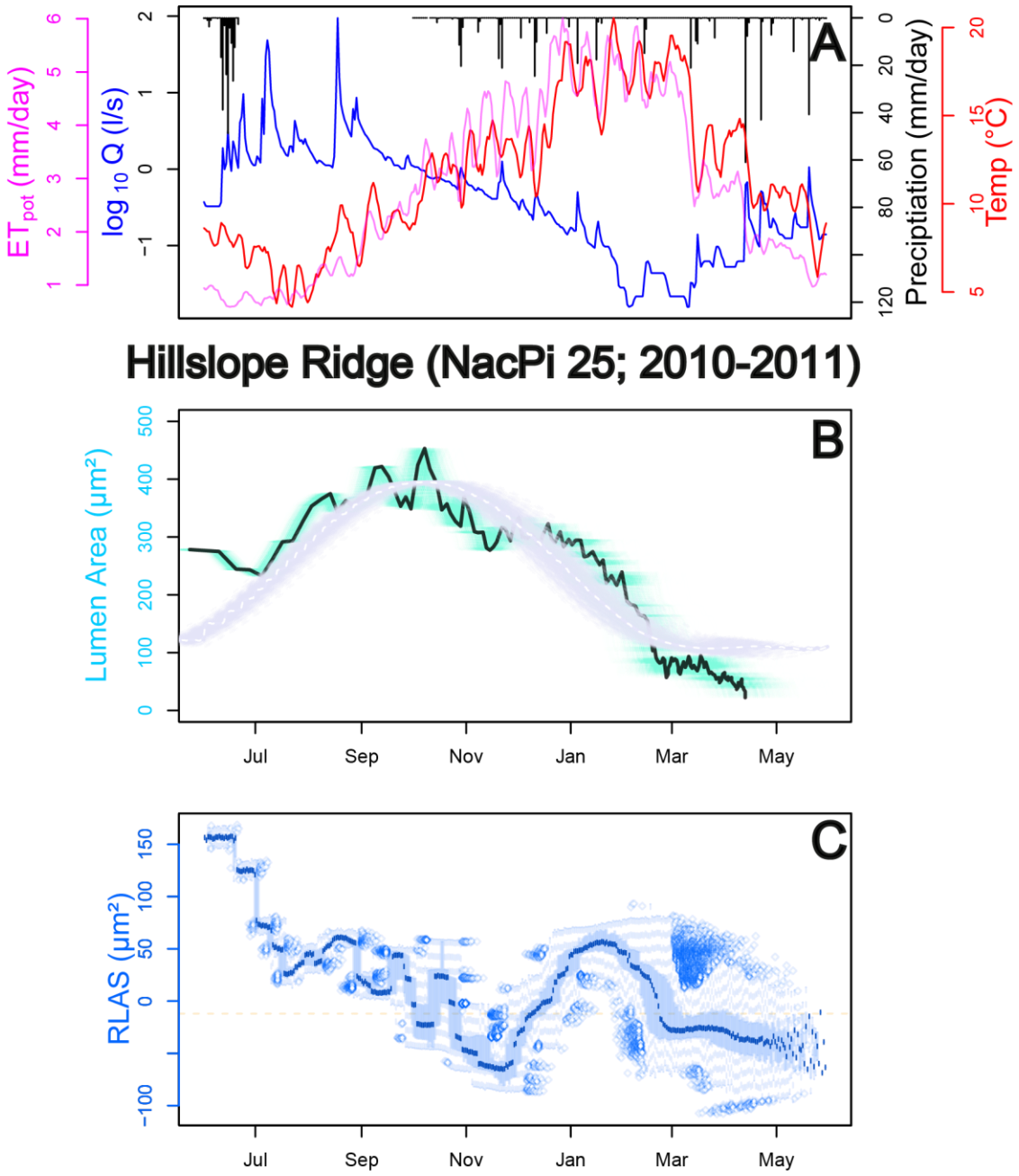


**Supplementary Figure 4.** Wood anatomy of NacPi25 for the 2010-11 growing season; See Supplementary Figure 3 for caption.

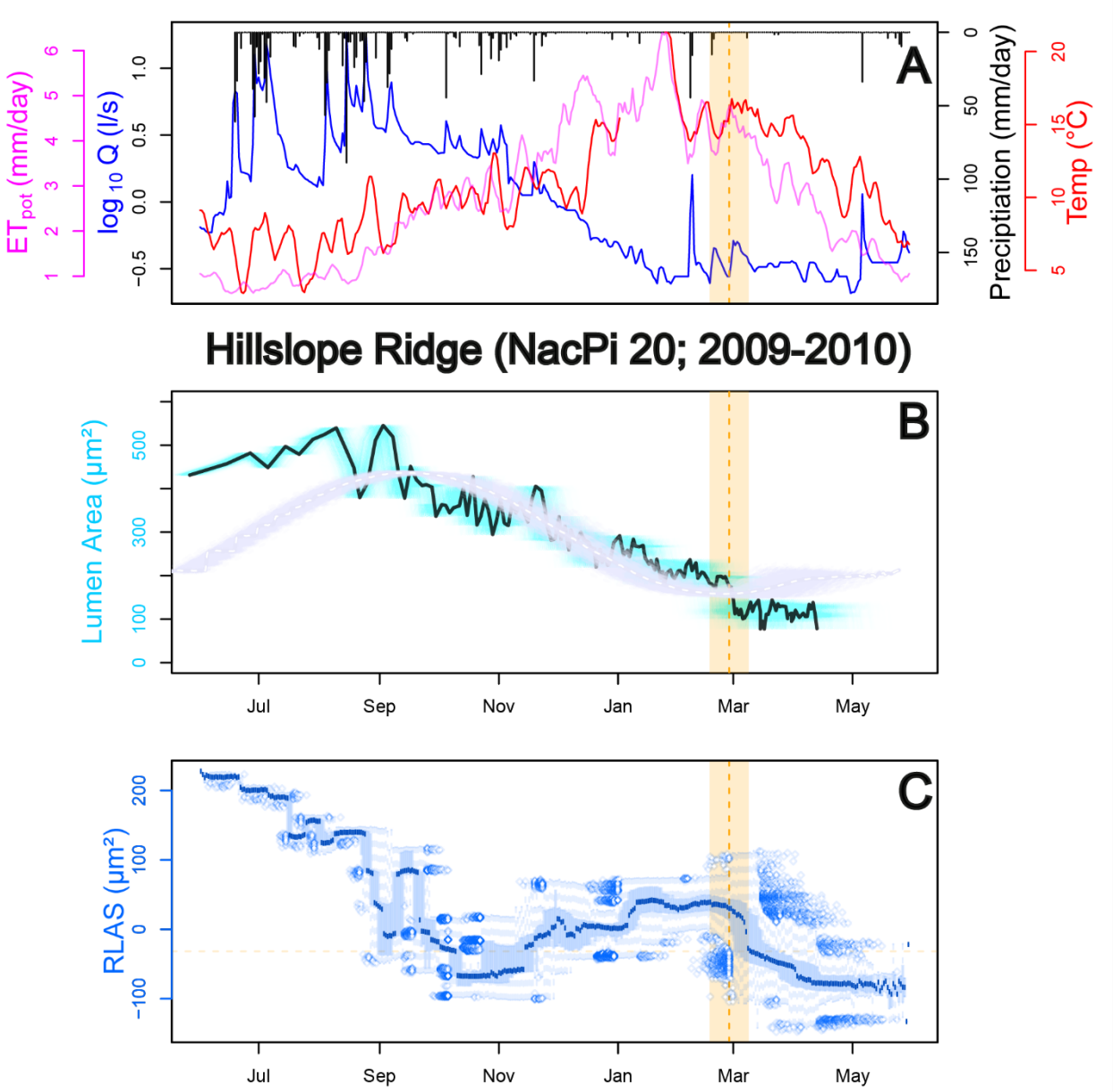


**Supplementary Figure 5.** Wood anatomy of NacPi20 for the 2009-10 growing season; See Supplementary Figure 3 for caption.

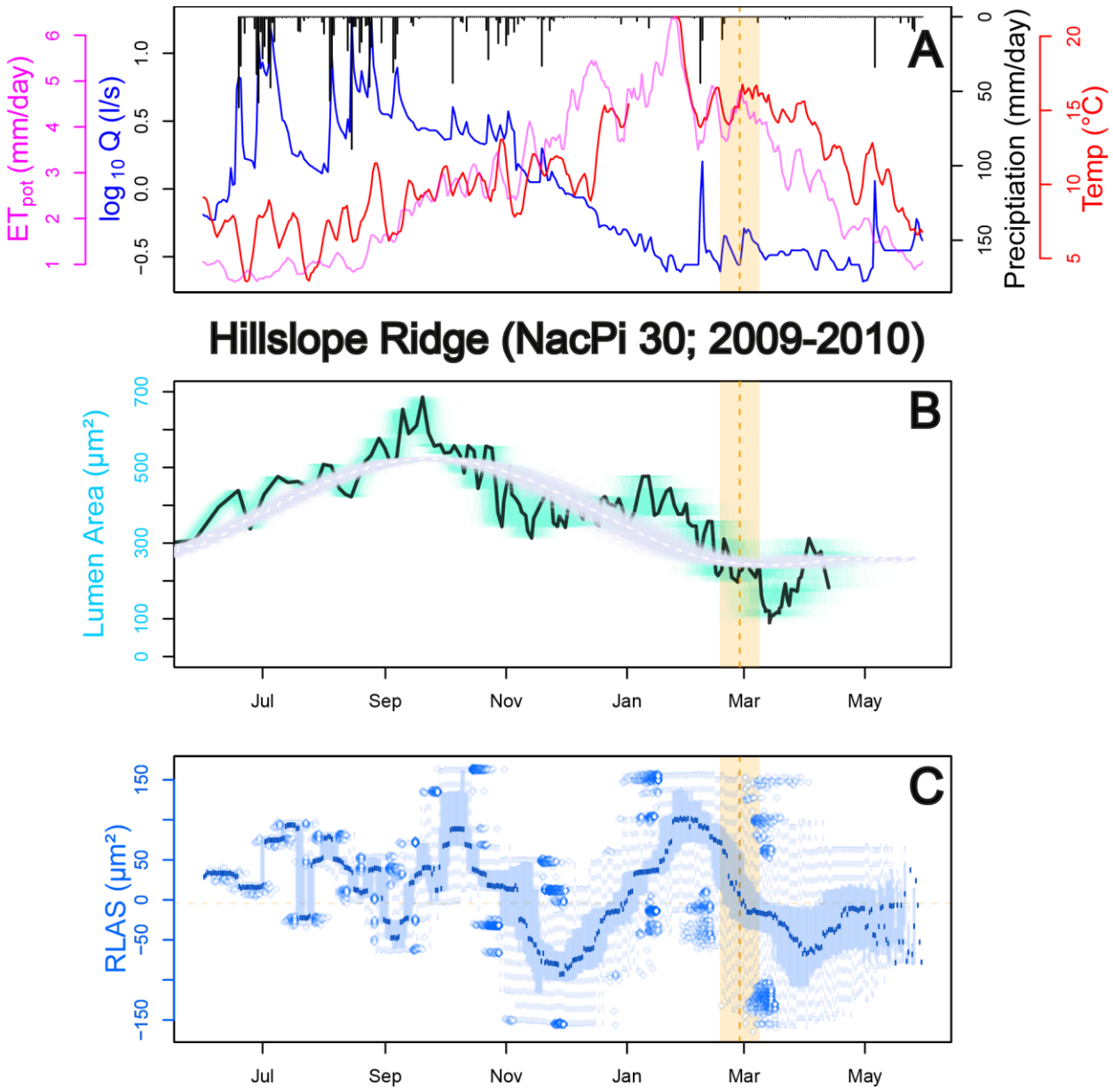


**Supplementary Figure 6.** Wood anatomy of NacPi30 for the 2009-10 growing season; See Supplementary Figure 3 for caption.

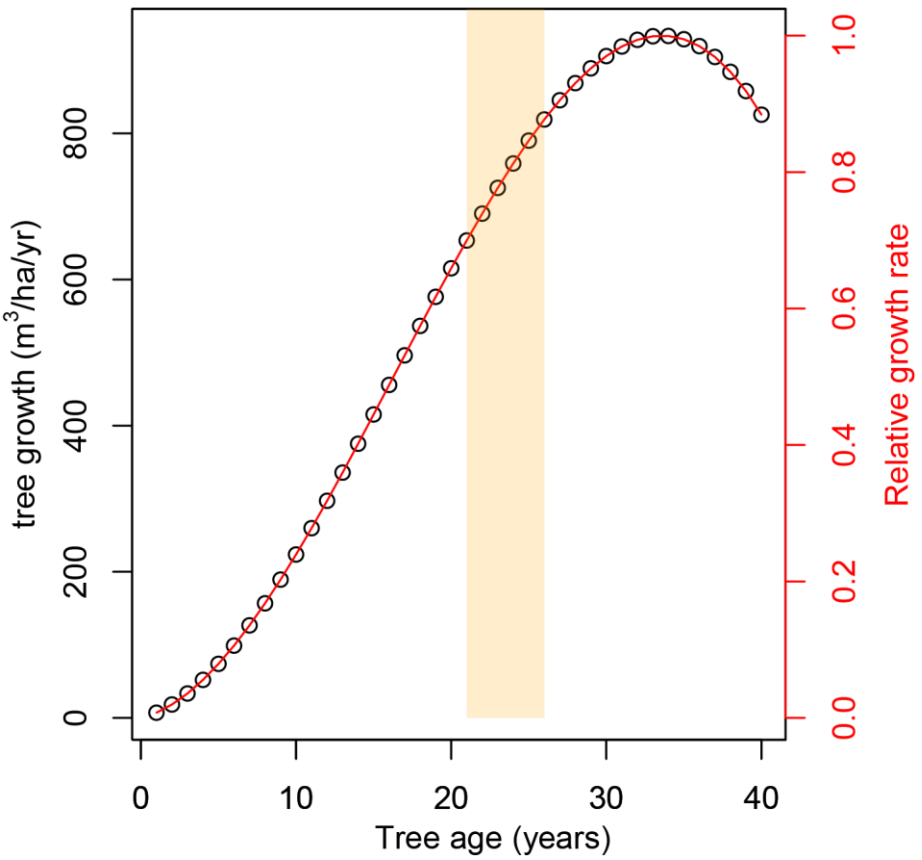


**Supplementary Figure 7.** Modeled absolute ($m^3$/ha/yr) and relative growing rates of *Pinus radiata* D.Don [*Cerda Vargas and Nuñez Sandoval*, 1996]. The orange bar indicates the time period covered by the intra-annual $\boldsymbol{\delta^{13}C_{OM}}$ samples.

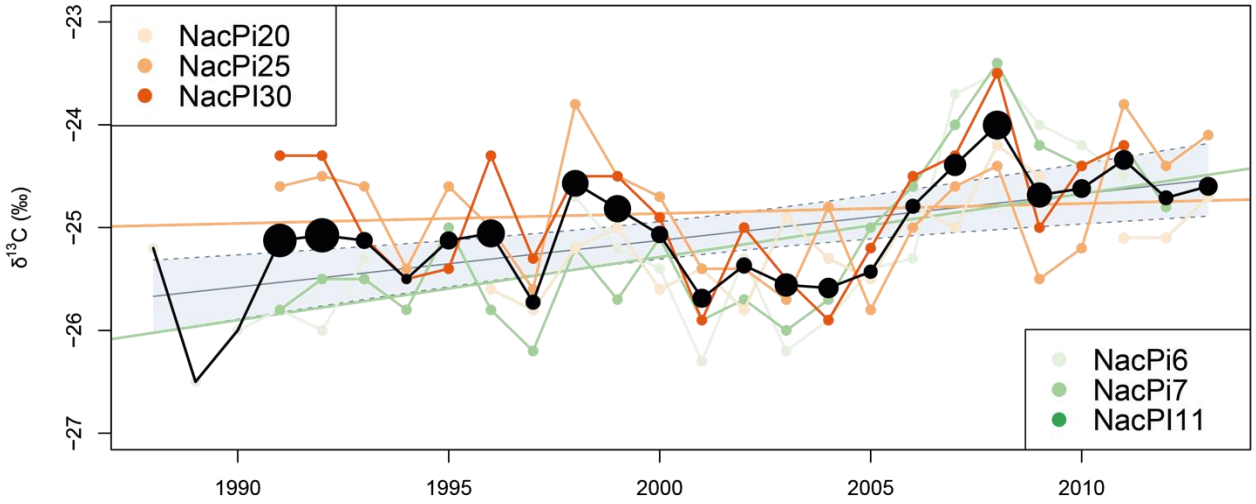


**Supplementary Figure 8.** Inter-annual $\boldsymbol{\delta^{13}C_{OM}}$ cellulose measurements of the cored trees separated into upper (orange) and lower slope (green) locations (y = 0.045x – 25.71, $R^2$ = 0.39, p-value: 0.0008). The black lines correspond to the average with the dot size scaled with the standard deviation. Note: The first three entries are only provided by NacPi6 and thus follow the black line. Grey area represents the confidence bounds (95%) with the centered median model fit.

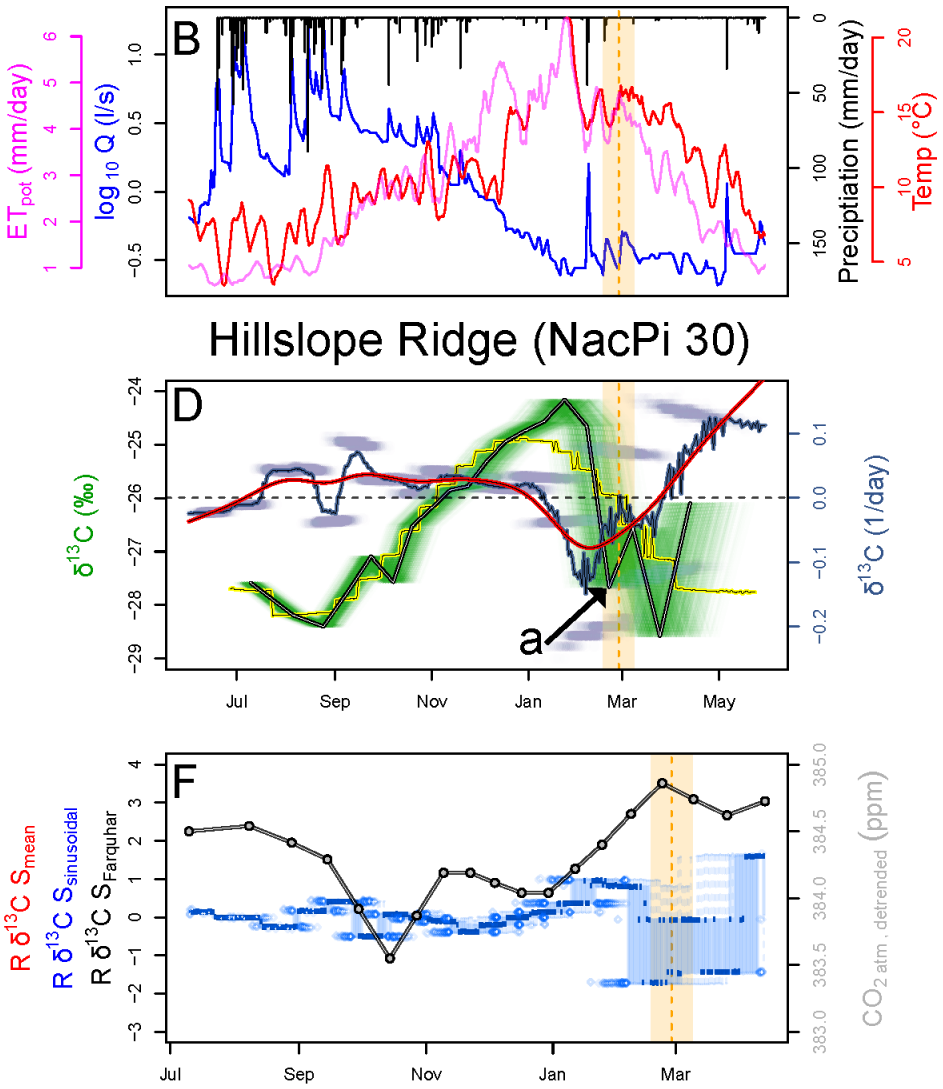


**Supplementary Figure 9.** Intra-annual $\boldsymbol{\delta^{13}C_{OM}}$ fractionation of NacPi30 during the growing season 2009-2010. **b)**: Time series of discharge (on logarithmic scale) in blue, rainfall (black), air temperature (red), and potential evapotranspiration (pink). Data on streamflow discharge, rainfall, and air temperature from S.A. ; potential evapotranspiration from Nicodahue catchment (#8362001) of CAMEL-CL data [*Alvarez-Garreton et al.*, 2018]. The orange bars and dashed lines mark the earthquake date ±10 days. **d)** The black curve is the median of all MC-modeled time series of $\boldsymbol{\delta^{13}C_{OM}}$ (n = 10,000, green array of curves) of NacPi30. Daily rates of $\boldsymbol{\delta^{13}C_{OM}}$ change are violet points with violet solid line showing medians and red dashed line showing spline regression. The yellow curves are medians of *n*=10,000 MC- sinusoidal–models per sampled cellulose increments. **f)** Residual $\boldsymbol{\delta^{13}C_{OM}}$ signals (R$\boldsymbol{\delta^{13}C_{OM}}$S); grey and red bars are $\boldsymbol{\delta^{13}C_{OM}}$-residuals to of the Farquhar-models and residuals between observed $\boldsymbol{\delta^{13}C_{OM}}$-values and the annual mean, respectively. The blue boxplot time series are daily $\boldsymbol{\delta^{13}C_{OM}}$-residuals of sinusoidal model. The grey dotted curves are de-trended atmospheric $CO_2$ (ppm) measured at Baring Head, New Zealand [*Keeling et al.*, 2001].

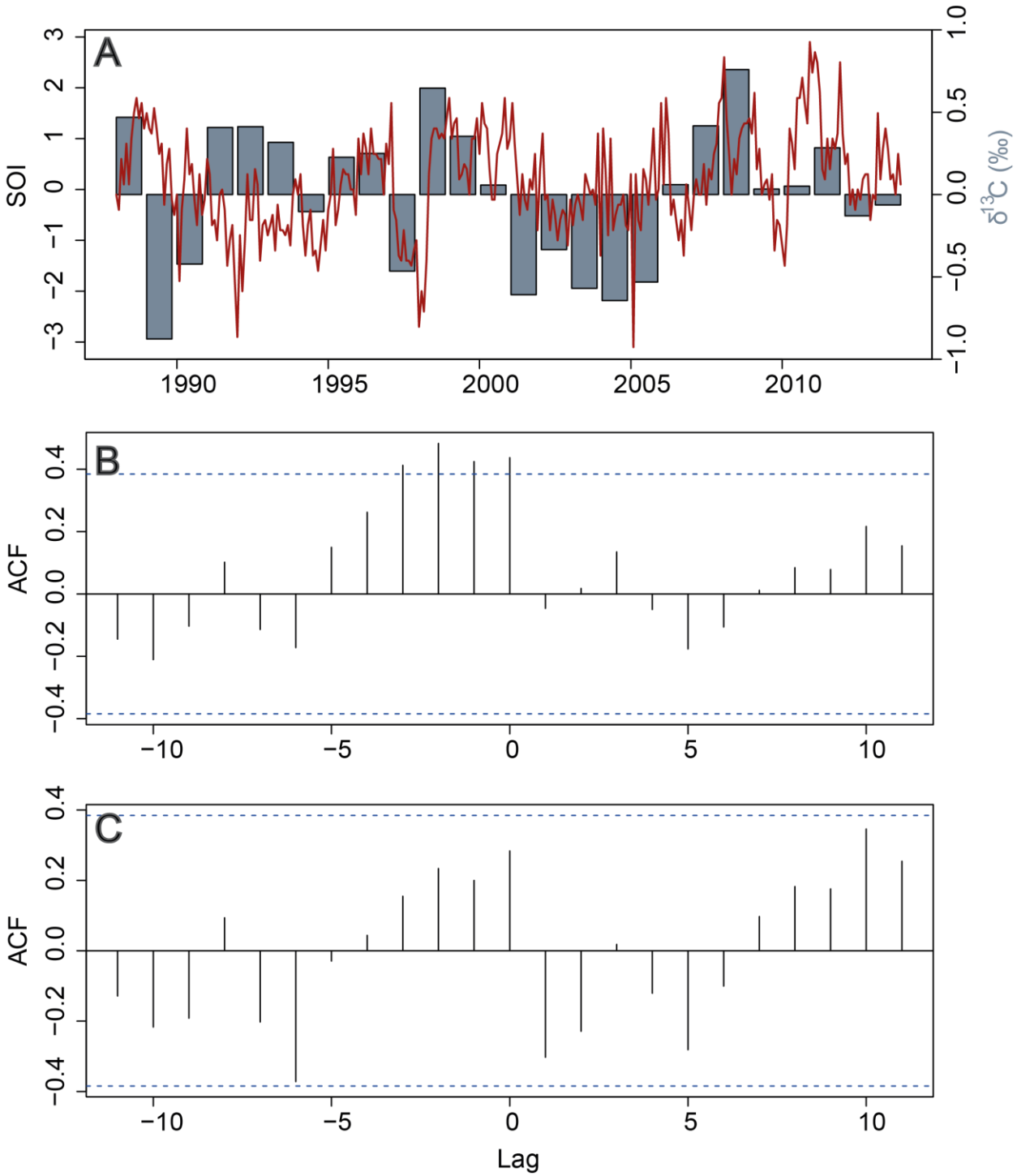


**Supplementary Figure 10.** Time series of $\delta^{13}C_{OM}$-model residuals and Southern Oscillation Index (SOI). **a)** Grey bars correspond to the model residuals to account for detrended atmospheric $CO_2$ concentrations (see Supplementary Figure 2), the red line depicts the monthly Southern Oscillation Index SOI (downloaded from https://www.ncdc.Noaa.gov /teleconnections/enso/indicators/soi, 02/14/2020). **b)** Cross correlation between annually resolved $\delta^{13}C_{OM}$ values and SOI; C: cross correlation between model

residuals of linear trend (Supplementary Figure 2) and SOI. We used the R package rsoi (https://cran.r-project.org/web/packages/rsoi/rsoi.pdf)

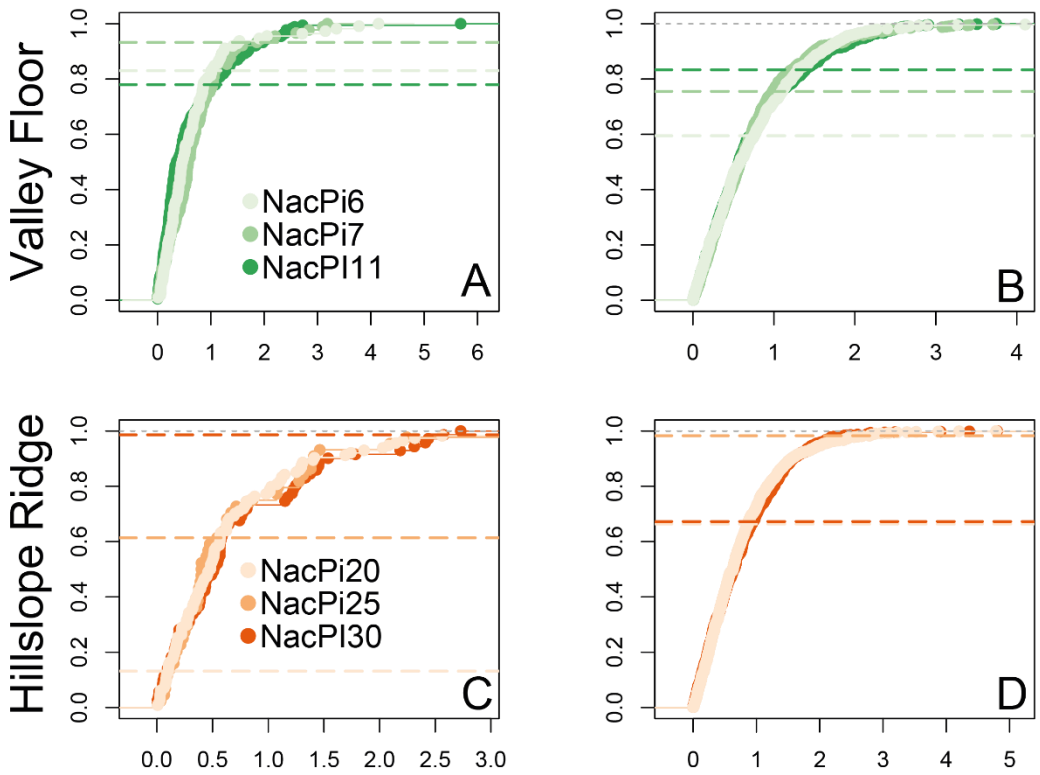


**Supplementary Figure 11.** Empirical cumulative density functions of absolute, standardized model residuals for $\boldsymbol{\delta^{13}C_{OM}}$ (**a, c**) and lumen area (**b, d**) for the valley bottom and hillslope ridge. All data are standardized to the specific tree. Green colors refer to valley floor, reddish color to ridge. Marked horizontal lines show the empirical frequencies for the residuals assigned to the first sample-date of the earthquake for $\boldsymbol{\delta^{13}C_{OM}}$. See Supplementary Table 8 for values.

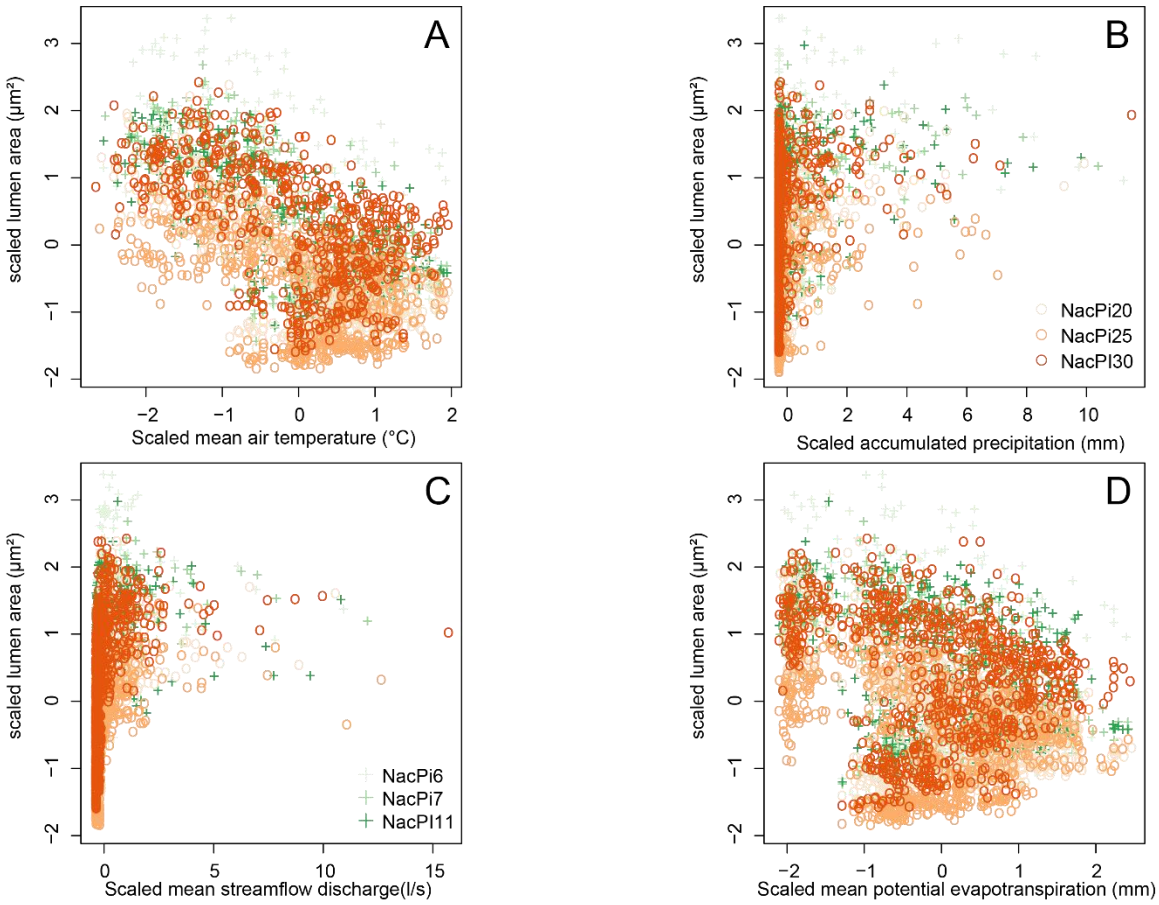


**Supplementary Figure 12.** Scaled lumen area (µm$^2$) as a function of (A) mean air temperature (°C), (B) accumulated precipitation (mm), (C) mean streamflow discharge (l/s), and (D) mean potential evapotranspiration (mm). Air temperature, precipitation, streamflow and potential evapotranspiration are estimated for the time periods needed for cell formation.

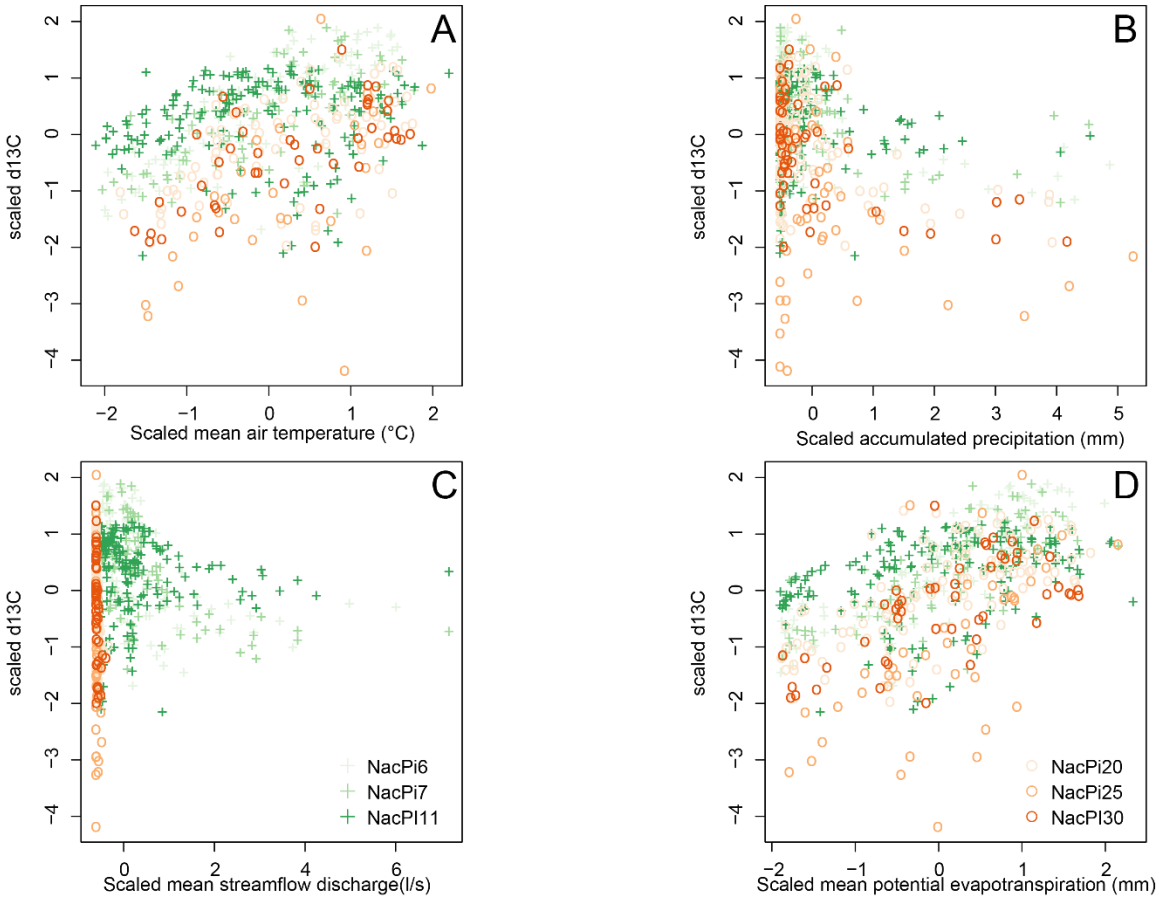


**Supplementary Figure 13.** Scaled $\boldsymbol{\delta^{13}C_{OM}}$ as a function of (A) mean air temperature (°C), (B) accumulated precipitation (mm), (C) mean streamflow discharge (l/s), and (D) mean potential evapotranspiration (mm). Air temperature, precipitation, streamflow and potential evapotranspiration are estimated for the time periods needed for cell formation.

| Month | Cumulative DBH growth (cm) | Cumulative height growth (cm) |
|---|---|---|
| Jun | 2.5 | 3.8 |
| Jul | 5.8 | 7.8 |
| Aug | 11.8 | 13.8 |
| Sep | 22.3 | 25.8 |
| Oct | 34.3 | 41.3 |
| Nov | 44.3 | 59 |
| Dec | 56.3 | 74 |
| Jan | 67.3 | 82 |
| Feb | 78.1 | 88 |
| March | 89.1 | 92.1 |
| Apr | 95.1 | 95.9 |
| May | 98.6 | 99.9 |

**Supplementary Table 1.** Field measurements of DBH and tree height growth from Nacimiento Pinus radiata plantation forests, data provided by Mininco.

| Year | NacPi6 | NacPi7 | NacPi11 | NacPi20 | NacPi25 | NacPi30 |
|---|---|---|---|---|---|---|
| 2006/07 | 17 | - | - | 26 | - | - |
| 2007/08 | 14 | 31 | 42 | 17 | - | 22 |
| 200809 | 25 | 32 | 32 | 28 | - | 23 |
| 2009/10 | 25 | 34 | 35 | 28 | 11 | 20 |
| 2010/11 | 27 | 17 | 35 | 19 | 10 | 13 |
| 2011/12 | 21 | 21 | 51 | 14 | 16 | 15 |
| 2012/13 | 14 | - | 28 | - | 9 | 17 |
| Σ | 143 | 135 | 223 | 132 | 46 | 110 |

**Supplementary Table 2.** Number of $\boldsymbol{\delta^{13}C_{OM}}$ samples for each tree and growing season

| Site | $ridge_{pre}$ | $ridge_{post}$ | $valley_{pre}$ | $valley_{post}$ |
|---|---|---|---|---|
| $R^2$ | 0.78 | 0.46 | 0.63 | 0.83 |
| Individual Tree | 11.9 | 3.5 | 12.9 | 6.0 |
| Accum. Precipitation | 4.8 | 16.3 | 9.0 | 24.9 |
| Max. Precipitation | 5.3 | 7.8 | 3.4 | 8.9 |
| Mean Precipitation | 4.6 | 9.4 | 2.7 | 7.5 |
| Solar Radiation | 32.1 | 24.8 | 40.7 | 29.7 |
| Mean Air Temperature | 23.0 | 16.2 | 8.6 | 6.3 |
| Mean Discharge | 18.3 | 21.9 | 22.7 | 16.7 |

**Supplementary Table 3.** Model performance ($R^2$) and relative variable importance of the $\delta^{13}C_{OM}$-Boosted Regression Tree models. Note: Mean discharge recorded at the catchment outlets during said period. Note: Solar radiation here as "Potential Incoming Solar Radiation" and derived from topography [*Conrad et al.,* 2015], see also Supplementary Table 5.

| Growing season | Mean °C | Accumulated rainfall (mm) |
|---|---|---|
| 2008-9 | 10.95±3.39 | 756 |
| 2009-10 | 10.37±3.25 | 1177 |
| 2010-11 | 10.77±3.36 | 888 |
| 2011-12 | 11.51±3.84 | 1062 |
| 2012-2013 | 11.51±3.72 | 670 |

**Supplementary Table 4.** Mean annual air temperatures (°C) and accumulated rainfall registered at the nearest meteorological stations at Pichún. The long term mean annual air temperature is 11.0 ± 3.8 °C (01/1979-12/2016) (CAMEL-CL, *Alvarez-Garreton et al.* [2018]).

| Tree ID | Potential solar radiation ($kWh/m^2\,yr^{-1}$) |
|---|---|
| NacPi6 | 1975.5±111.3 |
| NacPi7 | 19.94.6±120.4 |
| NacPi11 | 2137.6±32.3 |
| NacPi20 | 2007.0±12.5 |
| NacPi25 | 2079.5±11.0 |
| NacPi30 | 2055.9±15.5 |

**Supplementary Table 5.** Modeled annual potential incoming solar radiation [*Böhner and Antonić*, 2009; *Conrad et al.*, 2015], i.e. the all-year sum of direct and diffuse insolation, within a 10-m buffer around each cored tree during the period 01/01/2010-12/31/2010. Calculation has been performed at a 2h resolution; lumped atmospheric transmittance is assumed as 70%; local sky factor was calculated using the 5m DEM [*Conrad et al.*, 2015]. Values were calculated using the potential incoming solar radiation algorithm implemented in SAGA-GIS (http://www.saga-gis.org/saga_tool_doc/2.2.2/ta_lighting_2.html). The algorithm recognized three main governing factors: (1) relative orientation of the Earth in relation to the sun, (2) clouds and other atmospheric inhomogeneity, such as dust, and (3) topography.

| Proxy | Growing season | NacPi6 | NacPi7 | NacPi11 | NacPi20 | NacPi25 | NacPi30 |
|---|---|---|---|---|---|---|---|
| Early wood (%) | 2008-2009 | 48.63 | 53.38 | 51.13 | 59.25 | 45.38 | 67.63 |
| | 2009-2010 | 53.88 | 83.88 | 76.25 | 63.38 | 57.00 | 73.63 |
| | 2010-2011 | 68.38 | 78.50 | 79.38 | 71.25 | 60.38 | 73.38 |
| | 2011-2012 | 64.63 | 71.44 | 59.00 | 62.63 | 50.00 | 72.75 |
| | 2012-2013 | 62.63 | 59.38 | 60.38 | 82.13 | 47.56 | 77.63 |
| Mean early wood (µm) | 2008-2009 | 402.82 | 312.29 | 403.13 | 310.67 | 259.47 | 435.03 |
| | 2009-2010 | 424.48 | 392.54 | 383.07 | 284.34 | 323.18 | 449.07 |
| | 2010-2011 | 406.72 | 404.41 | 447.86 | 318.72 | 317.37 | 421.21 |
| | 2011-2012 | 423.13 | 456.61 | 386.23 | 329.04 | 309.04 | 403.69 |
| | 2012-2013 | 559.00 | 407.79 | 383.44 | 318.16 | 243.17 | 405.45 |
| Mean tree ring width (mm) | 2008-2009 | 2.59 | 5.60 | 5.92 | 2.63 | 1.84 | 3.75 |
| | 2009-2010 | 3.83 | 4.86 | 5.04 | 4.00 | 2.06 | 4.37 |
| | 2010-2011 | 3.89 | 3.65 | 5.87 | 3.79 | 1.73 | 2.76 |
| | 2011-2012 | 4.18 | 2.78 | 5.77 | 2.58 | 1.84 | 2.23 |
| | 2012-2013 | 3.09 | 2.42 | 8.88 | 2.33 | 1.89 | 2.30 |
| Number of cells | 2008-2009 | 110.00 | 215.00 | 210.00 | 125.00 | 90.00 | 130.00 |
| | 2009-2010 | 150.00 | 160.00 | 170.00 | 170.00 | 80.00 | 140.00 |
| | 2010-2011 | 140.00 | 120.00 | 200.00 | 165.00 | 75.00 | 100.00 |
| | 2011-2012 | 140.00 | 80.00 | 200.00 | 120.00 | 90.00 | 80.00 |
| | 2012-2013 | 110.00 | 80.00 | 300.00 | 100.00 | 80.00 | 80.00 |
| Mean lumen area ($\mu m^2$) | 2008-2009 | 254.74 | 242.10 | 311.37 | 236.12 | 156.76 | 353.38 |
| | 2009-2010 | 303.14 | 372.55 | 353.56 | 233.96 | 227.62 | 395.35 |
| | 2010-2011 | 334.44 | 363.37 | 410.83 | 261.01 | 223.46 | 358.38 |
| | 2011-2012 | 352.82 | 387.95 | 315.86 | 255.47 | 191.17 | 332.23 |
| | 2012-2013 | 415.42 | 315.32 | 316.41 | 288.24 | 171.80 | 350.27 |

**Supplementary Table 6.** Absolute mean (µm) and relative (%) early wood and number of cells, tree ring width (mm), and lumen area (µm2) averaged from *n*=8 paths for the sampled trees during respective growing seasons.

| Year | NacPi6 | NacPi7 | NacPi11 | NacPi20 | NacPi25 | NacPi30 |
|---|---|---|---|---|---|---|
| 1987/88 | -25.2 | NO DATA | NO DATA | NO DATA | NO DATA | NO DATA |
| 1988/89 | -26.5 | NO DATA | NO DATA | NO DATA | NO DATA | NO DATA |
| 1989/90 | -26 | NO DATA | NO DATA | NO DATA | NO DATA | NO DATA |
| 1990/91 | -25.8 | -25.8 | NO DATA | -24.6 | -24.3 | NO DATA |
| 1991/92 | -26 | -25.5 | NO DATA | -24.5 | -24.3 | NO DATA |
| 1992/93 | -25.3 | -25.5 | NO DATA | -24.6 | -25.1 | NO DATA |
| 1993/94 | NO DATA | -25.8 | NO DATA | -25.4 | -25.5 | -25.3 |
| 1994/95 | NO DATA | -25 | NO DATA | -24.6 | -25.4 | -25.5 |
| 1995/96 | NO DATA | -25.8 | -25.6 | -25 | -24.3 | -24.6 |
| 1996/97 | NO DATA | -26.2 | -25.8 | -25.6 | -25.3 | -25.7 |
| 1997/98 | -24.7 | -25.2 | -25.2 | -23.8 | -24.5 | -24 |
| 1998/99 | -25.2 | -25.7 | -25 | -24.5 | -24.5 | -24 |
| 1999/00 | -25.4 | -25.1 | -25.6 | -24.7 | -24.9 | -24.7 |
| 2000/01 | -26.3 | -25.9 | -25.4 | -25.4 | -25.9 | -25.2 |
| 2001/02 | -25.3 | -25.7 | -25.8 | -25.4 | -25 | -25 |
| 2002/03 | -26.2 | -26 | -24.9 | -25.7 | -25.5 | -25 |
| 2003/04 | -25.9 | -25.7 | -25.3 | -24.8 | -25.9 | -25.9 |
| 2004/05 | -25.4 | -25 | -25.5 | -25.8 | -25.2 | -25.7 |
| 2005/06 | -25.3 | -24.6 | -24.8 | -25 | -24.5 | -24.5 |
| 2006/07 | -23.7 | -24 | -25 | -24.6 | -24.3 | -24.7 |
| 2007/08 | -23.5 | -23.4 | -24.2 | -24.4 | -23.5 | -25 |
| 2008/09 | -24 | -24.2 | -24.5 | -25.5 | -25 | -24.9 |
| 2009/10 | -24.2 | -24.4 | NO DATA | -25.2 | -24.4 | -24.9 |
| 2010/11 | -24.5 | -24.2 | -25.1 | -23.8 | -24.2 | -24.3 |
| 2011/12 | NO DATA | -24.8 | -25.1 | -24.4 | NO DATA | -24.5 |
| 2012/13 | NO DATA | NO DATA | -24.7 | -24.1 | NO DATA | -25 |

**Supplementary Table 7.** Annual $\boldsymbol{\delta^{13}C_{OM}}$ values. NO DATA refers to no measured data available for the respective growing season.